ORIGINAL PAPER

**M. Zhang · E. K. H. Salje · R. C. Ewing · P. Daniel
T. Geisler**

Applications of near-infrared FT-Raman spectroscopy in metamict and annealed zircon: oxidation state of U ions

Abstract We report a near-infrared Fourier-transform (FT) Raman spectroscopic method to characterize the electronic transitions of U ions and the alpha-decay damage in natural zircon. The application is demonstrated by analyzing metamict and annealed zircons from Sri Lanka. The data from crystalline zircon reveal a relatively sharp spectral feature appearing near 2733 cm^{-1} in Stokes spectra with a laser excitation of 1064 nm. The feature is assigned as signals related to the previously reported U^{5+} absorption near 6668 cm^{-1}. With increasing self-irradiation dose, the feature shows a systematic decrease in intensity, accompanied by a gradual development of a broad feature between 3000 and 3400 cm^{-1}. On heating for 1 h, the U^{5+} feature shows an increase in intensity starting near ~ 700 K for partially metamict zircon, whereas for highly damaged zircon the first recovery of the feature takes place near 1000 K, accompanied by a decrease in the radiation-induced broad band. The changes observed in the present study reflect the variations of local environments of U ions in natural zircon during metamictization and thermal annealing.

M. Zhang (✉) · E. K. H. Salje
Department of Earth Sciences, University of Cambridge
Downing Street, Cambridge, CB2 3EQ, UK
e-mail: mz10001@esc.cam.ac.uk
Tel: (44) 01223–333411
Fax: (44) 01223–333450

R. C. Ewing
Department of Nuclear Engineering and Radiological Sciences
Department of Geological Sciences
University of Michigan, Ann Arbor, MI 48109-2104, USA

P. Daniel
Laboratoire de Physique de l'Etat Condensé,
UPRES A CNRS n°6087
Université du Maine – Faculté des Sciences
Av. Olivier Messiaen - 72085 Le MANS Cedex 9,
France

T. Geisler
Mineralogisches Institut, Universität Münster,
Corrensstr. 24, 48149 Münster, Germany

Introduction

Natural zircon (ZrSiO$_4$) frequently occurs in igneous rocks and sediments. It crystallizes in a tetragonal symmetry (D$_{4h}^{19}$ or $I4_1/amd$). The crystal structure of zircon constitutes of a chain of alternating, edge-sharing SiO$_4$ tetrahedra and ZrO$_8$ triangular dodecahedra extending parallel to the crystallographic c axis. Zircon commonly contains several thousand ppm U and Th and is thus an important mineral geochronometer. During geological periods, the α-decay of the U and Th and their daughter products causes damage to the crystal structure of zircon and a transformation from a crystalline to an amorphous (metamict) state (Ewing 1994; Weber et al. 1998; Salje et al. 1999; Ewing et al. 2003).

In natural zircon, the structure-incorporated U ions, in fact, exist as defects in the crystal, and their characteristic spectral feature is sensitive to the alteration of the local structural configurations. Analyzing and investigating the behaviour of U ions in metamictization gives information on the impact of radiation on crystal defects and the radiation-induced structural changes (Zhang et al. 2002). Although the U concentrations in zircon can be as high as a few thousands of ppm, their presence can hardly be detected using common vibrational spectroscopy. Instead, the presence of U ions and their structural changes can be revealed in the near-infrared (IR) region, where the electron energy levels of U ions are located. In natural zircon, U atoms replace Zr atoms and occupy the Zr^{4+} site. The Zr^{4+} site is non-centrosymmetric, D_{2d}, thus electronic transitions for paramagnetic impurities (e.g. U ions) are possible. Experimental and theoretical work has been performed to gain an understanding of the energy levels of U ions. U^{4+} and U^{5+} spectra of U-doped synthetic and heated natural zircon have been obtained (Judd and Runciman 1976; Richman et al. 1967; Mackey et al. 1975; Vance and Mackey 1974;

1975; 1978). The U energy levels can be labelled in terms of five irreducible representations of the D_{2d} point group: four singlets Γ_1, Γ_2, Γ_3, Γ_4 and one doublet Γ_5. The degenerate $5f2(SL)J$ terms split into 70 levels: $16\Gamma_1 + 9\Gamma_2 + 12\Gamma_3 + 12\Gamma_4 + 21\Gamma_5$, i.e. 49 singlets Γ_1, Γ_2, Γ_3, Γ_4 and 21 doublets Γ_5. In a recent near-IR study of metamict and heated zircon, Zhang et al. (2002) reported the observation of a systematic change of the spectral profile of absorption bands of electron transitions of U between 4000 and 13 000 cm^{-1}, which was explained as radiation-related ionization. Investigating radiation-induced changes in the valence states of ions in metamict materials is of importance, as these changes may play a significant role in the micro-structural evolution of irradiated materials and result in modifications of other physical properties (Ewing 2001). Consequently, the mobility of the defects may be affected, and eventually the chemical durability and dissolution rate may be altered. This may affect the leaching behaviour of natural zircon and the related diffusion processes. In addition, the modification of valence states can change the local configurations associated with hydrous components and give rise to new sites for OH species in zircon. Therefore, to characterize and understand the changes of valence states of incorporated ions in natural zircon are of importance, because element migration in metamict materials is a critical issue for candidate materials proposed for the immobilization and stabilization of nuclear waste forms.

We undertook this study as a part of our recent studies of the metamictization and recrystallization of zircon using far-IR, mid-IR, near-IR and Raman spectroscopy (Zhang et al. 2000a–c; Zhang and Salje 2001; Zhang et al. 2002, 2003). Zhang et al. (2003) reported that radiation leads to an alteration of the oxidation states of U ions whereby the tetravalent state is preferable in radiation-damaged zircons. Recrystallization and structural recovery at high temperatures result in complex oxidation/reduction reactions. Firstly, we wished to find a simple FT-Raman method to characterize and analyze spectral features related to different types of U-ion signals, and to further investigate the behaviour of the U-ion bands of natural zircons in metamictization and thermal annealing. Our second goal was to further explore possible Raman applications to easily detect and characterize the formation of amorphous materials in metamict zircon. Although Raman spectroscopy has been successfully used to characterize zircon and to estimate the degree of radiation damage, the application is mainly based on the radiation-induced change of linewidth and frequency of the phonon bands (particularly the Si–O stretching near 1008 cm^{-1}) of the crystalline phase of zircon (Nasdala et al. 1995, 2001, Zhang et al. 2000a, c; Geisler et al. 2001; Geisler 2002). Unfortunately, because the amorphous materials in metamict zircon produce very low Raman scattering, this essentially makes the method unsuitable for analyzing highly damaged zircon that contains a few remaining crystal-

line domains. Even for zircon crystals with intermediate degrees of damage, the coexistence of both the crystalline and the amorphous materials and the band broadening makes the determination of spectral parameters (e.g. band linewidth) of the Raman vibrational bands through curve-fitting procedures difficult. We wished to use near-IR FT-Raman spectroscopy, through measuring bands associated with U ions, to trace characteristic bands from both crystalline and amorphous domains. To our knowledge, this FT-Raman application is the first of its kind.

The idea of using near-IR FT-Raman spectroscopy to study absorption bands related to electronic transitions is based on laser-induced fluorescence (Lakowicz 1983; Guilbault 1990; Ferraro and Nakamoto 1994). Since laser-induced fluorescence often produces unwanted features in vibrational Raman spectra and makes data interpretation complicated, it is usually avoided in Raman vibrational studies. In this study, however, we took advantage of this commonly unwanted feature to explore the electronic transitions of U ions in metamict zircons. For instance, the near-IR U^{5+} absorption band near 6668 cm^{-1} observed by near-IR spectroscopy could appear near 2730 cm^{-1} (in terms of Raman shift) in Stokes spectra when the excitation of 1064 nm is used. We shall show in this contribution that the fluorescence spectra of this absorption can be easily obtained and used for the analysis of radiation damage and tracing the variation of oxidation states of U ions. The method could also be useful for studying and characterizing U ions in natural zircons.

Experimental

The zircon samples used in this study are mainly crystals from Sri Lanka. They were chosen because of their gem quality and low chemical impurities. The work of Geisler and Schleicher (2000) has indicated that gem crystals from Sri Lanka are virtually unaltered by geological events. These samples have been well characterized previously by electron microprobe, X-ray, TEM, Raman and far-IR, mid-IR and near-IR (Murakami et al. 1991; Ellsworth et al. 1994; Salje et al. 1999; Zhang et al. 2000a, b, c). The studied crystals showed variations of colours (straw, dark straw, pale yellow, yellow, green-yellow, green), similar to the Sri Lankan zircons used by Woodhead et al. (1991). However, black or very dark brown samples with a high degree of damage were excluded from our Raman measurements, because they produced strong backgrounds which prevented us from analyzing the data quantitatively. Powdered samples studied by Zhang and Salje (2001) were used in most measurements, as the U-ion spectra from crystalline zircon showed orientation preference (Zhang et al. 2002). However, several samples were measured in the form of crystals, because we wished to use them for other single-crystal measurements. To reduce any potential effect of orientation dependence on the results, for each crystal spectra were randomly recorded along different orientations and the data were then averaged. Several zircon crystals were oriented using their external morphology for polarized Raman measurements. All annealing experiments were carried out in N_2 atmosphere in a vertical furnace. Fresh samples were used for the annealing at each temperature and annealed samples were quenched onto lab benches in air. In this study, the self-irradiation dose (based on the age of ~570 Ma for the zircon and its U and Th contents) (Holland and Gottfried 1955; Murakami

et al. 1991) for the natural zircon crystals has been used to characterize the degree of damage. At present, this appears the best parameter to use in determining the extent of damage, and will allow us to assess the relative changes in the crystalline and metamict domains of the zircon crystals.

FT-Raman spectra were recorded in the region of 80–3800 cm^{-1} using a Bruker IFS 66v spectrometer adapted with a Bruker FRA 106 FT-Raman accessory. A silicon-coated calcium fluoride beam-splitter, an Nd:YAG laser with radiation of 1064 nm, and a liquid-nitrogen-cooled, high-sensitivity Ge detector were employed. The spectrum (with an instrumental resolution of 2 cm^{-1}) was recorded with a laser power of 50 mW and a back-scattering geometry. Two dispersive Raman spectrometers were also used in this study. Polarized conventional Raman spectra between 1500 and 8000 cm^{-1} were recorded in a back-scattering with a T64000 Jobin-Yvon ISA multichannel Raman spectrometer attached to an Olympus FX40 microscope (objective ×50 LF) and coupled with a liquid-nitrogen-cooled CCD detector. A confocal hole coupled with the microscope was adjusted to a medium value in order to enhance the axial resolution. The lateral spot size was about 2–5 μm. A triple subtractive configuration (gratings of 1800 lines mm^{-1}) of the spectrometer was selected in order to improve the resolution. In order to check for possible luminescence signals, the laser line of 514.5 nm excitation of a coherent argon-krypton ion laser was used. The entrance slit widths were adjusted to obtain an instrumental resolution of 2 cm^{-1}. Unpolarized conventional Raman spectra (between 150 and 1100 cm^{-1}) of annealed zircons were recorded using LabRam micro-Raman spectrometer. A 632-nm Ne-He laser was used for the excitation. A CCD detector, a grating (1800 grooves mm^{-1}), and a 50× ultra-long working-distance objective were coupled with a free-sample-space microscope.

Results and discussion

### Effects of radiation damage on FT-Raman spectrum of zircon

The effect of radiation damage on FT-Raman spectra of zircon between 2000 and 3800 cm^{-1} is illustrated in Fig. 1a. The spectra of natural zircon are normalized by the highest intensity in the region of 2000–3800 cm^{-1} to reveal details for better comparison. In crystalline natural zircon, a strong peak near 2733 cm^{-1} was observed. However, this feature did not appear in the FT-Raman spectrum of a synthetic pure zircon. Its presence in natural zircon is associated with the absorption band near 6668 cm^{-1} in near-IR absorption spectra reported previously (Vance and Mackey 1974; Zhang et al. 2002, 2003). The absorption was assigned as an U^{5+} band (Vance and Mackey 1974, 1975). Judd and Runciman (1976) proposed that it could be attributed to $\Gamma_6 \rightarrow \Gamma_6$ and $\Gamma_7 \rightarrow \Gamma_7$ transitions. Experimental results (Vance and Mackey 1978) confirmed this prediction and revealed that there was no accidental degeneracy in the ground state of U ions. The fundamental vibrations of zircon crystal can produce multi-phonon bands in this region, which have been recorded near 2700 cm^{-1} by the IR absorption method (Woodhead et al. 1991; Zhang et al. 2002). However, their contributions to the FT-Raman spectra in Fig. 1a must be very weak or ignorable, because the FT-Raman feature near 2733 cm^{-1}

shows a much higher intensity than those of the fundamental vibrational bands located between 100 and 1100 cm^{-1} in a weakly damaged sample (Fig. 1b). The multi-phonon bands are generally one or two orders weaker than the fundamental bands. This clearly shows that the 2733 cm^{-1} feature is not mainly caused by multi-phonon bands. Several sharp and weak lines also appear between 2800 and 2900 cm^{-1} in crystalline zircons. They are probably associated with the sharp and weak IR absorption lines between 6550 and 6620 cm^{-1} revealed in absorption spectra at low temperatures (Zhang et al. 2003).

On increasing the degree of damage, the sharp U^{5+} feature gradually shifts to ~2745 cm^{-1} at self-irradiation dose of 3.5×10^{18} α-events g−1 (Fig. 1a). This is consistent with the observations of Zhang et al. (2003), who reported that the U^{5+} absorption band near 6668 cm^{-1} shifted to ~6652 cm^{-1}. We also noted that the 2733 cm^{-1} band in the FT-Raman spectra exhibited a systematic decrease in intensity and became almost undetectable at doses higher than 7.5×10^{18} α-events g−1. This was accompanied by the development of a broad spectral feature located between 3000 and 3400 cm^{-1} that appeared in partially metamict samples (Fig. 1a). The real shape of the broad feature could be somehow distorted because its peak position is close to the frequency limit of the detection of the FT-Raman measurements. In contrast to a systematic decrease in intensity for the feature near 2733 cm^{-1}, this broad feature shows an increase in intensity with increasing degree of radiation damage. In comparison with the Raman bands of the fundamental vibrations of zircon (below 1010 cm^{-1} in Fig. 1b), the relatively strong intensities of these additional features (Fig. 1a, b) indicate that they are not associated with multi-phonon bands. This broad feature is also not the result of the self-absorption or black-body absorption that commonly appears in FT-Raman of black samples, because black samples were excluded from this study and FT-Raman spectra from black samples show very different patterns. In general, the intensity of self-absorption depends on the position of the sample in the sampling chamber, and it commonly decreases dramatically on increasing the distance from the beam focus point. We measured several samples at different focus positions, and the results do not support the idea of possible self-absorption. In addition, sample thickness plays a significant role in self-absorption, but this was not observed in our measurements. Other potential causes that could produce bands in the frequency region of 3000–3400 cm^{-1} are hydrous species, U spectra reported by Zhang et al. (2002) or unknown electron transitions due to chemical impurities. We shall show in a later section that OH and H$_2$O are unlikely to be responsible for the broad features.

To obtain quantitative information on the spectral changes of the 2733 cm^{-1} band as well as the broad band peaked near 3265 cm^{-1} as a function of degree of radiation damage, we analyzed the relative intensity ratios

Fig. 1 Effect of radiation damage on near-infrared FT-Raman spectra of zircon: **a** between 2000 and 3800 cm^{-1}; **b** between 100 and 3800 cm^{-1}. The spectra from natural zircons are normalized by the highest intensity between 2000 and 3600 cm^{-1} to show details. The self-irradiation doses are in the units of 10^{18} α-events g−1. The features near 2733 cm^{-1} are due to the U^{5+} bands centred near 6668 cm^{-1} in near IR spectra. (Zhang et al. 2002)
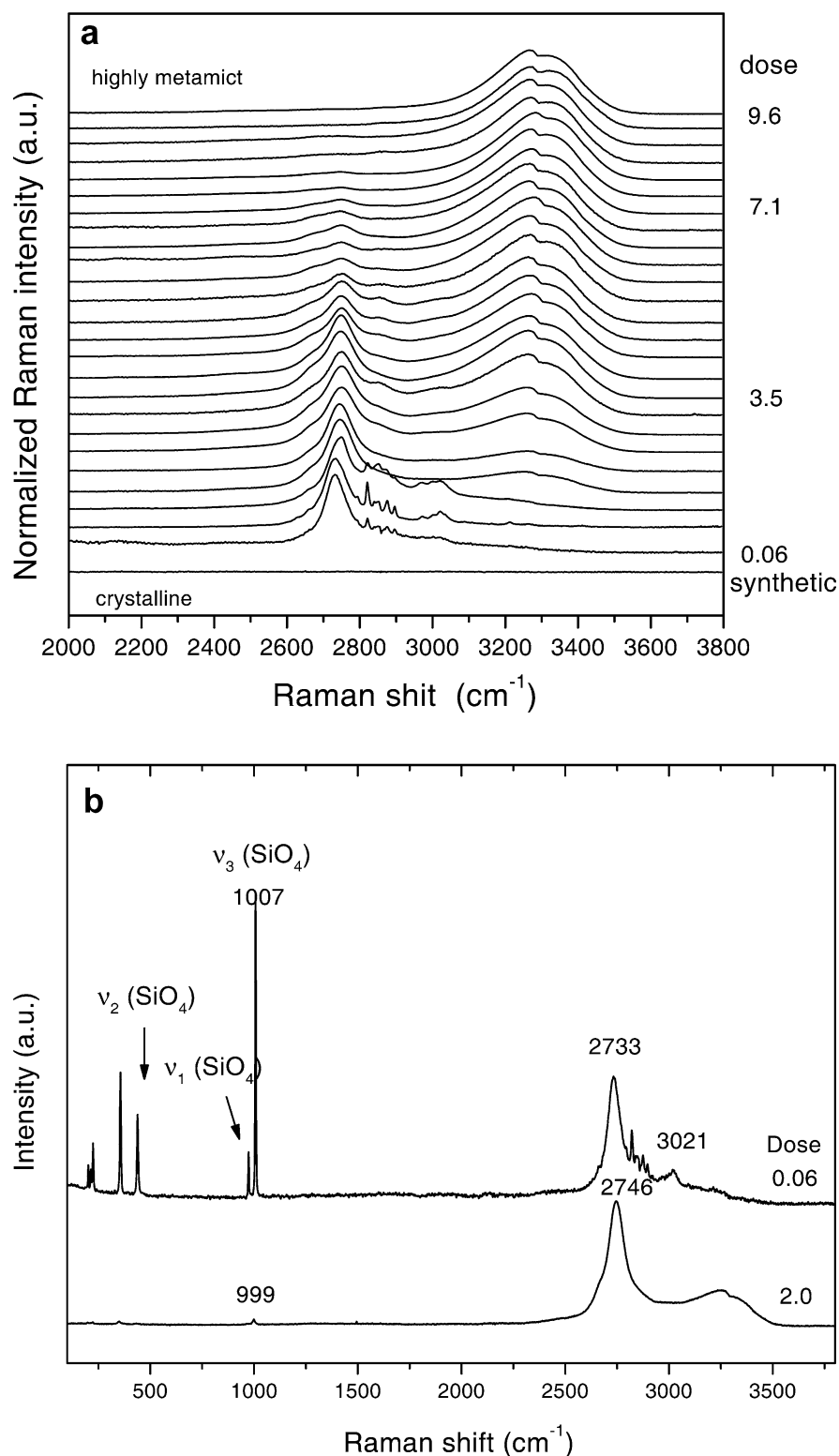
associated with the two features (Fig. 2). The data in Fig. 2 define sigmoidal curves, which reach saturation at a dose $>9 \times 10^{18}$ α-decay event g−1. The fraction data of the amorphous phase in metamict zircon, obtained by X-ray diffraction (Ríos et al. 2000), ^{29}Si NMR (Farnan and Salje 2001) and mid IR (Zhang and Salje 2001), are also shown in Fig. 2 for comparison. It is surprising to see that the relative intensity $[I_{3265}/(I_{2745} + I_{3265})]$ of the broad feature gives rise to a dose-dependence close to that of the fraction of the amorphous phase. The results appear to indicate that the observed changes of the bands are associated with the volume of the crystalline

Fig. 2 Intensity ratios [$I_{2745}/(I_{2745} + I_{3265})$ and $I_{3265}/(I_{2745} + I_{3265})$] (*solid symbols*) and the fraction of amorphous phase as a function of dose (*open symbols*). The IR results are from Zhang and Salje (2001), the X-ray diffraction data (XRD) from Ríos et al. (2000) and ^{29}Si nuclear magnetic resonance (NMR) data from Farnan and Salje (2001). The *solid line* is the function $f = 1 - e^{-BaD}$ where D is radiation dose and $B_a = 2.7(3) \times 10^{-19}$ g is the amount of amorphous material produced per alpha-recoil (Ríos et al. 2000). The *dash line* is a visual guide
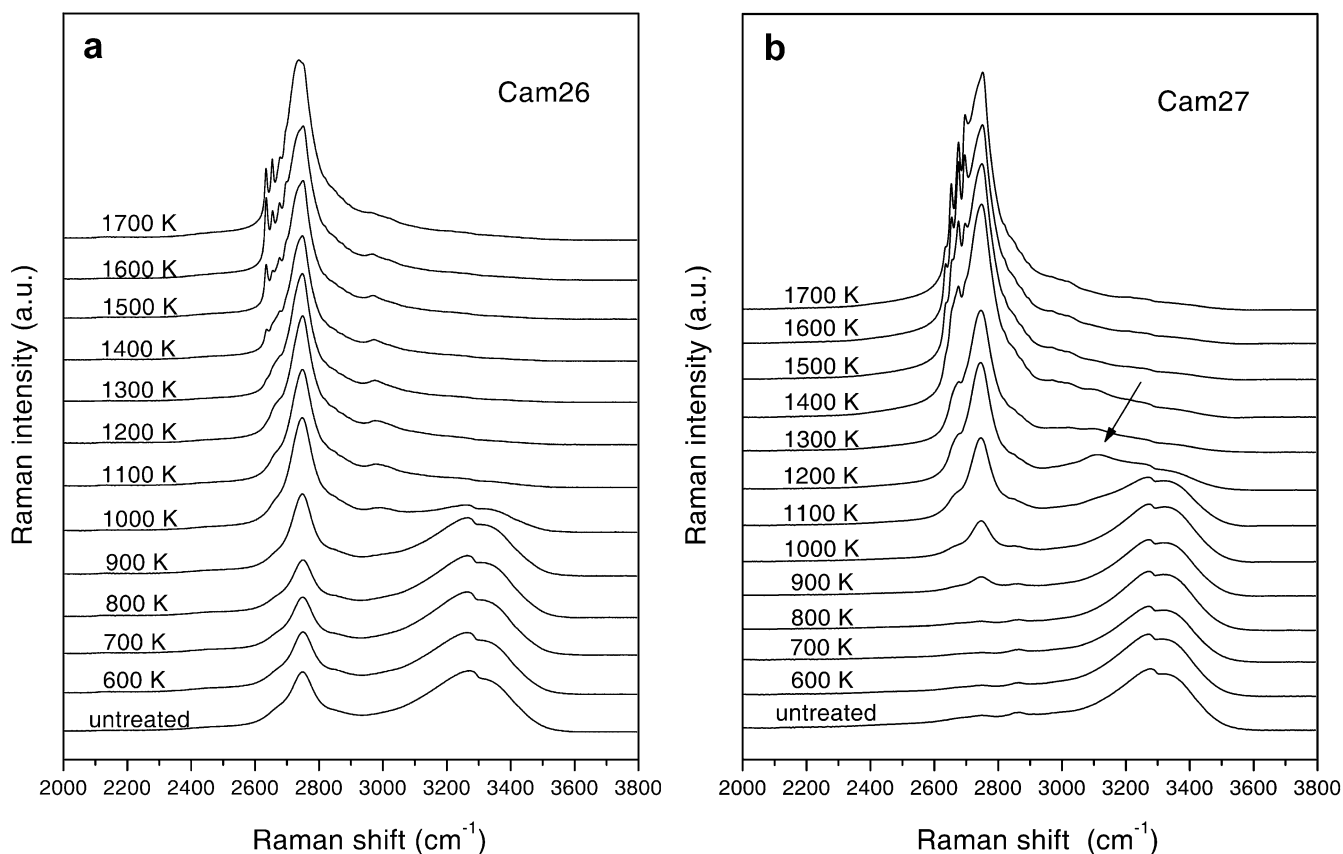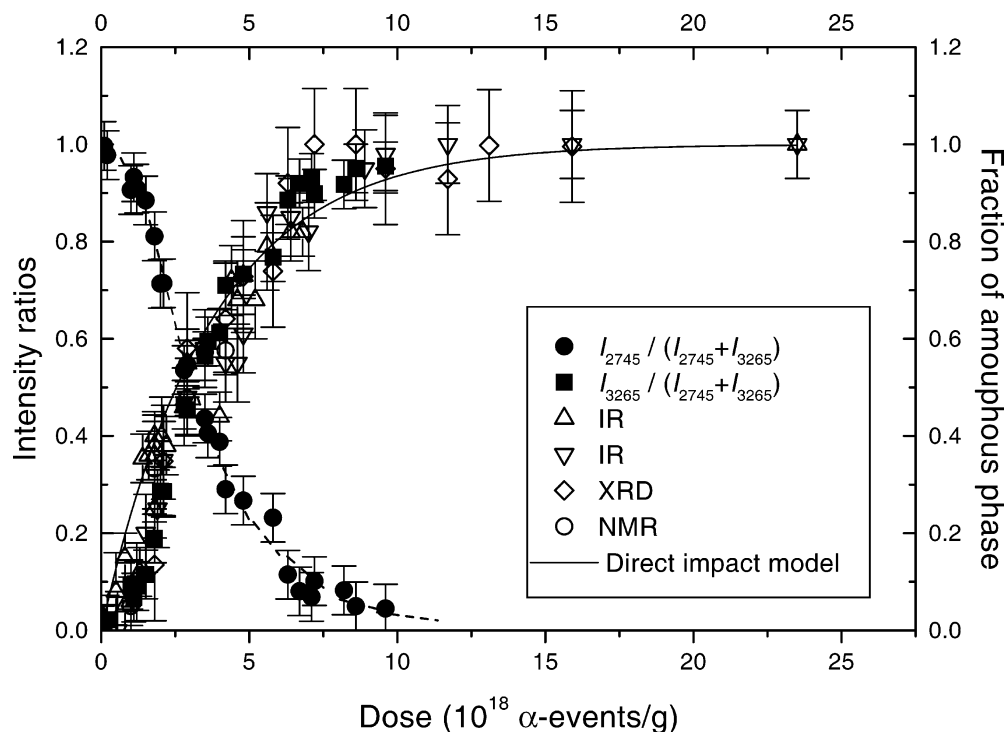
Fig. 3 FT-Raman spectra of damaged zircon annealed at temperatures between 600 and 1700 K for 16 h. **a** Sample Cam26 (dose = 2.9×10^{18} α-events g^{-1}); and **b** sample Cam27 (dose = 5.6×10^{18} α-events g^{-1})

and amorphous material. In our measurements, the bands associated with the amorphous material can be detected at very low doses (less than 1×10^{18} α-events

g^{-1}). This essentially supports direct impact damage in zircon (Ríos et al. 2000) and is consistent with the hypothesis that amorphization is produced in cascades. The data can be potentially used to estimate the relative damage in zircons, although further work is necessary to refine our understanding of side effects of thermal annealing, hydrothermal alternation, weathering, high-pressure impact, alternation of charge states and growth conditions. The dramatic decrease in the U^{5+} band in metamictization (Fig. 1a) is consistent with our previous observation that radiation damage in zircon leads to changes in the oxidation state of U ions (Zhang et al. 2003).

Thermal annealing and recrystallization

Damaged zircons were isochronally annealed between 600 and 1800 K in an N_2 atmosphere in order to restore the crystal structure of zircon. Eight damaged samples with different degrees of damage were annealed at various temperatures. The typical spectra of two annealed samples (with doses of 2.9 and 5.6×10^{18} α-events g^{-1}, respectively) are shown in Fig. 3a and b. The effects of annealing are characterized by two types of systematic change. (1) On heating above $\sim$700 K, annealed zircons showed a systematic increase of the sharp feature near 2733 cm^{-1}, accompanied by a decrease of the broad

Fig. 4a,b FT-Raman intensity ratios of metamict zircon annealed between 600 and 1800 K. **a** $I_{2745}/(I_{2745} + I_{3265})$; **b** $I_{3265}/(I_{2745} + I_{3265})$
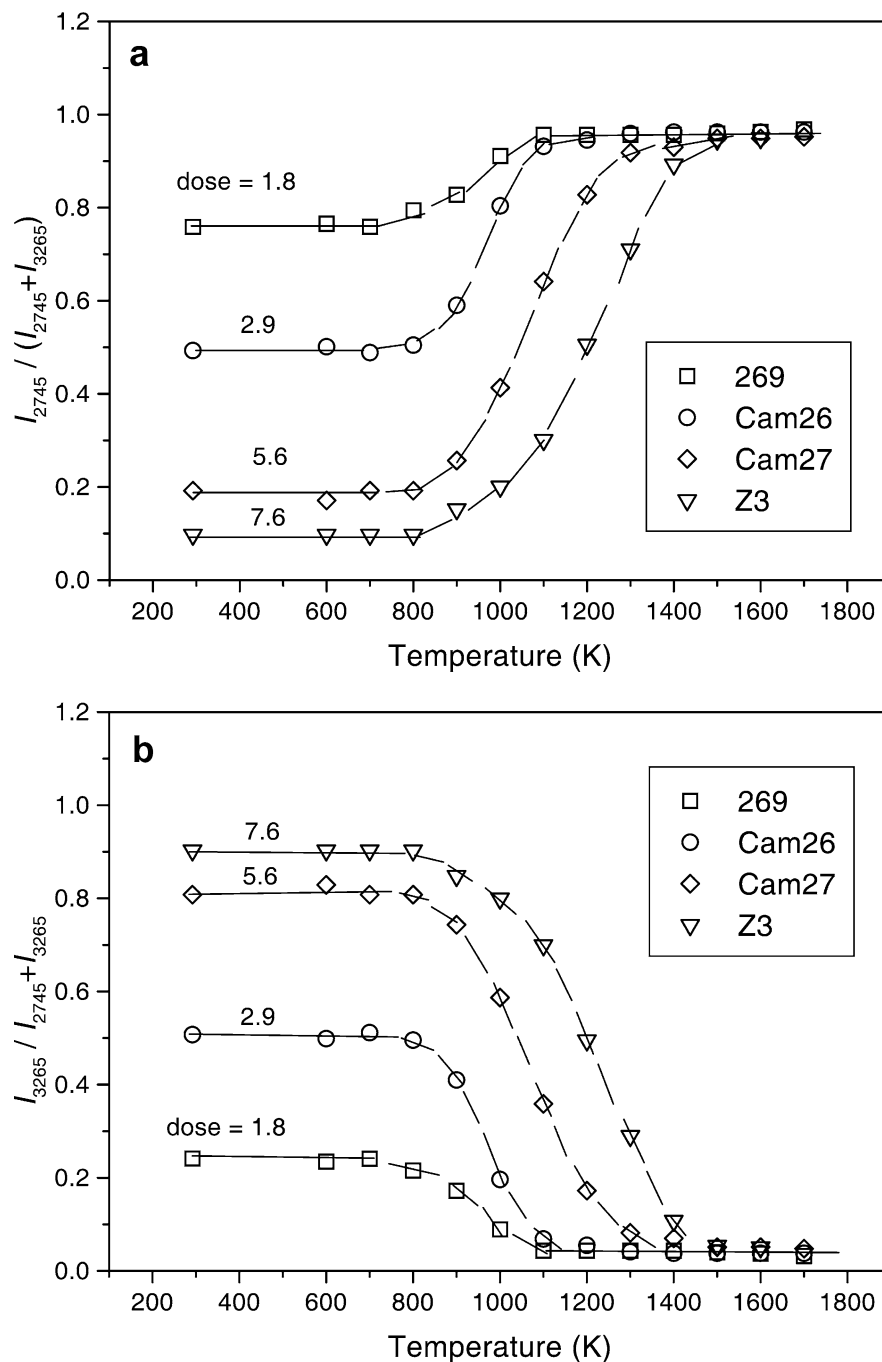
Fig. 5 Dispersive micro-Raman spectrum (632 nm excitation) of thermally decomposed zircon crystal (sample 157) annealed at 1200 K for 16 h. The bands indicated by t-ZrO_2 are the characteristic bands of tetragonal ZrO_2 produced by thermal decomposition
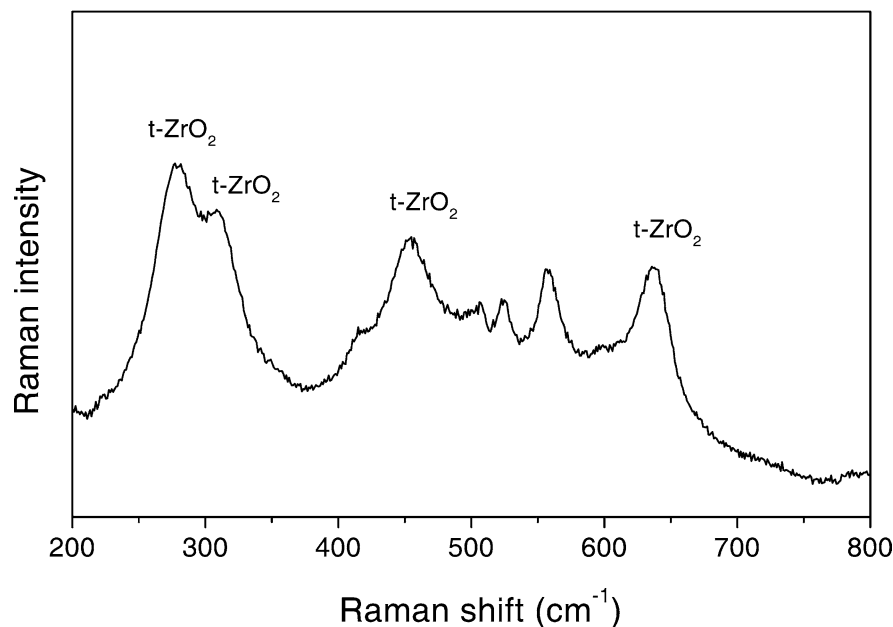
feature between 3000 and 3500 cm^{-1}. This is associated with annealing defects and the epitaxial growth seen in partially damaged samples (Zhang et al. 2000a, b). Intensity ratios were plotted in Fig. 4a and b to illustrate this change. The absence of the broad feature between 3000 and 3400 cm^{-1} in crystalline zircons and their disappearance during thermal annealing at high temperatures indicate that the signals are related to structure damage caused by radiation and associated with the radiation-induced amorphous materials in metamict zircon. (2) Zircons with different degrees of damage exhibited different thermal behaviour, and the recrystallization process depends on the degree of initial damage of the samples (Fig. 4a, b). The results support previous observations by X-ray diffraction (Ellsworth et al. 1994), electron microscopy (Capitani et al 2000) and vibration spectroscopy (Zhang et al. 2000a, b). In highly damaged zircon, annealing above 1100 K leads to decomposition into crystalline ZrO_2, which is evidenced by the occurrence of characteristic Raman bands of tetragonal ZrO_2 near 281, 311, 453 and 636 cm^{-1} (indicated by t-ZrO_2 in Fig. 5). Si-rich materials must coexist with ZrO_2 to maintain the original chemical composition of $ZrSiO_4$. Our observation of the decomposition of highly metamict zircon in annealing is consistent with previous results of thermally decomposed metamict zircons (Zhang et al. 2000a). In comparison with the Raman data of Zhang et al. (2000a), the lower frequency values and broader features of the tetragonal ZrO_2 observed in this study are probably due to the small size of the ZrO_2 particles. We noted that an extra feature near 3118 cm^{-1} (as indicated by an arrow in Fig. 3b) appeared in FT-Raman spectra of decomposed samples. However, this band was absent in untreated metamict zircon as well as in heated crystalline and weakly damaged zircon. We consider that this feature is

an indication of the thermally induced decomposition of $ZrSiO_4$.

The origin of the broad feature between 3000 and 3500 cm^{-1}

The formation of the broad features between 3000 and 3500 cm^{-1} in the FT-Raman spectra of metamict zircon is the result of metamictization in zircon as explained earlier, simply because they are absent in crystalline zircon (Fig. 1a) and because the features in metamict zircon disappeared after high-temperature annealing (Fig. 3a, 3b). At this stage, we can consider two possible causes responsible for the broad feature: new U-ion signals associated with the amorphized phase, or damage-induced OH and H_2O components (Woodhead et al. 1991; Zhang et al. 2002). These causes can be distinguished by two methods, (1) measuring Raman spectra with different wavelengths of laser excitations, and (2) comparing the IR absorption and FT-Raman data of samples dehydrated at high temperatures. If the feature is associated with laser-induced bands, one would expect that it may simply disappear or its peak position should show a dramatic variation when lasers with different wavelengths are used, whereas the frequencies (i.e. energy) of vibrational bands of OH and H_2O species are generally independent of excitation lasers. For the second method, spectral features of OH and H_2O species should disappear after dehydration.

Polarized conventional Raman spectra of a crystalline sample and an intermediately damaged zircon crystal (sample S4, dose = 4.8×10^{18} α-events g−1) were recorded with 514.5 -nm laser excitation (Fig. 6a, b). The reason for using polarized spectroscopy is that vibrational signals of the OH species of zircon show

orientation preference (e.g. Woodhead et al. 1991; Zhang et al. 2002), and we hoped to record all the possible O–H-stretching bands and to distinguish different contributions, although the outcome of the polarized spectroscopy did not appear very helpful in revealing OH and H_2O species. For the crystalline sample, the spectrum with the configuration of $y(zy)x$ [or $x(xy)x$ because of the uncertain x- and y-axis] revealed two sharp features near 2901 and 3194 cm^{-1} in the region of 3000–3400 cm^{-1}, whereas the $y(zz)y$ or $x(zz)z$ spectrum showed feature near 2801 cm^{-1} [In the standard notation $y(zy)x$ indicates that the incident light is directed along the crystal y-direction with z-polarization and the scattered light is observed along the y-axis with x-polarization]. These sharp bands are probably due to complex laser-induced bands with other chemical impurities, because they were not seen in FT-Raman data. Their frequency values are different from those of 3260 and 3335 cm^{-1} recorded in FT-Raman spectra. It is interesting that the bands near 2801, 2901 and 3194 cm^{-1} in the crystalline sample all shift to lower frequencies in the damaged crystal S4 (Fig. 6a, b) and this is probably due to the damage-induced defective structure of zircon. The different spectral features shown in spectra obtained with different laser excitations (Figs. 1a, 6a, b) favour the explanation that the broad feature between 3000 and 3400 cm^{-1} in FT-Raman data are not due to "hydrous species".

Our data from thermal annealing experiments further suggest that the broad feature in FT-Raman spectra is not mainly related to OH or H_2O. Although the presence of hydrous components in metamict zircon may potentially affect the FT-Raman features, the possible influences are not expected to be significant because Raman spectroscopy is less sensitive to hydrous species in comparison with IR spectroscopy. Small grains (0.2–0.5 mm) of a highly damaged zircon (sample 157, dose = 13.1×10^{18} α-events g^{-1}) were selected for

Fig. 6 Polarized dispersive Raman spectra (514.5 nm excitation): a crystalline zircon; b radiation-damaged zircon (sample S4, dose = 4.8×10^{18} α-events g^{-1}). In both a and b, the upper lines represent $x(xy)x$ or $y(zz)y$ (see texts for the details), the lower lines $x(zz)z$ or $y(zz)y$
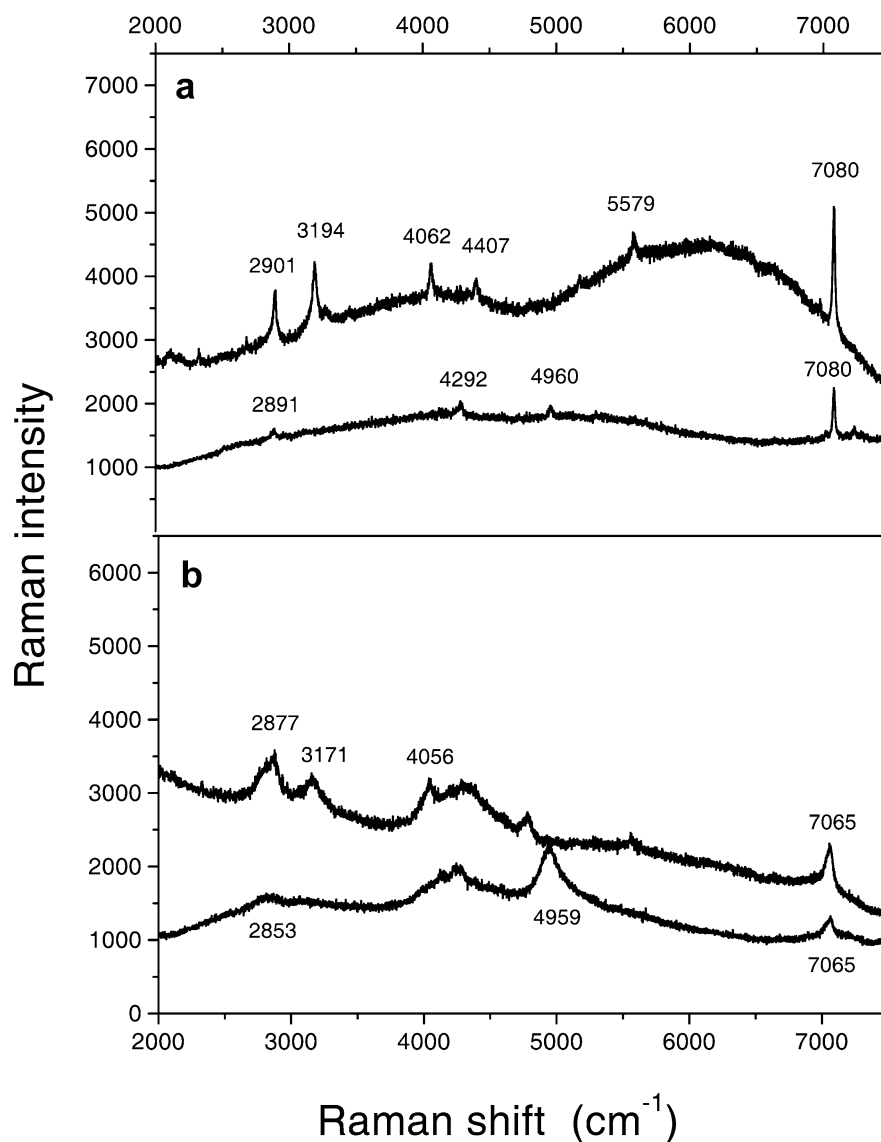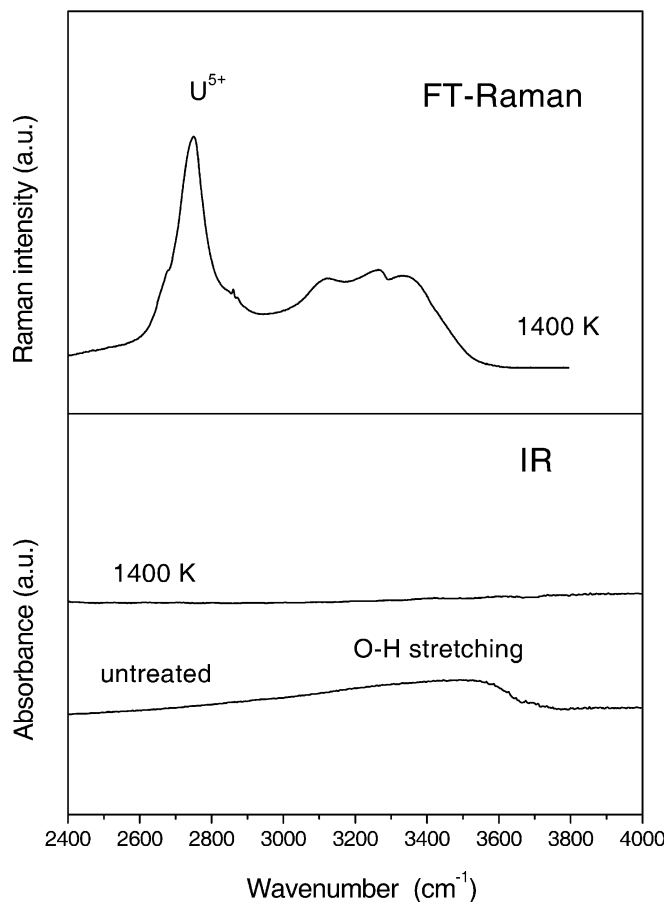
Fig. 7 IR and FT-Raman spectra of annealed highly metamict zircon (sample 157 with dose of 13.1×10^{18} α-events g^{-1}, annealed at 1400 K for 16 h)

high-temperature dehydration, because the structure recovery in highly damaged zircons is slow in comparison with weakly damaged samples (Zhang et al. 2000a, b, also see Fig. 3a, b) and the radiation-induced amorphous domains were expected to remain after dehydration took place. The small grains of the sample were individually annealed at different temperatures (1000, 1200 and 1400 K) for 16 h and then they were quenched to lab benches. The sample annealed at 1200 and 1400 K was essentially dehydrated, as indicated by the disappearance of the O–H absorption between 2500 and 3700 cm^{-1} in the IR spectra (Fig. 7). The flat lines between 2400 and 3700 cm^{-1} in samples annealed at 1400 K also indicated that the sample did not contain significant amounts of other hydrogen-related species. By contrast, the annealed sample still showed the broad feature between 3000 and 3400 cm^{-1} in the FT-Raman spectrum (Fig. 7). The observations confirm that hydroxyl and hydrous species are not responsible for the broad features shown in FT-Raman spectra of metamict zircon (Fig. 1a). We consider that they are likely to be related to the broad and weak feature absorption centred near 6040 cm^{-1} in U-ion spectra of damaged zircon revealed by near IR data (Zhang et al. 2002). The

frequency of the absorption feature is close to the calculated energy levels for U^{4+} ions (Richman et al. 1967; Vance and Mackey 1978).

Reference

Capitani GC, Leroux H, Doukhan JC, Ríos S, Zhang M, Salje EKH (2000) A TEM investigation of natural metamict zircons: structure and recovery of amorphous domains. Phys Chem Miner 27: 545–556
Ellsworth S, Navrotsky A, Ewing RC (1994) Energetic of radiation damage in natural zircon (ZrSiO4). Phys Chem Miner 21: 140–149
Ewing RC (1994) The metamict state: 1993—the centennial. Nuclear Instr Meth Phys Res (B) 91: 22–29
Ewing RC (2001) The design and evaluation of nuclear-waste forms: clues from mineralogy. Can Mineral 39: 697–715
Ewing RC, Meldrum A, Wang LM, Weber WJ, Corrales LR (2003) Radiation effects in zircon. Reviews in Mineralogy (in press)
Farnan I, Salje EKH (2001) The degree and nature of radiation damage in zircon observed by 29Si nuclear magnetic resonance. J Appl Phys 89: 2084–2090
Ferraro JR, Nakamoto K (1994) Introductory Raman spectroscopy. Academic Press, NewYork 370 pp
Geisler T (2002) Isothermal annealing of partially metamict zircon: evidence for a three-stage recovery process. Phys Chem Miner 29: 420–429
Geisler T, Schleicher H (2000) Improved U-Th-total Pb dating of zircons by electron microprobe using a new background modeling method and Ca as a chemical indicator of fluid-induced U–Th–Pb discordance in zircon. Chem Geol 163: 269–285
Geisler T, Pidgeon RT, van Bronswijk W, Pleysier R (2001) Kinetics of thermal recovery and recrystallization of partially metamict zircon: a Raman spectroscopic study. Eur J Miner 13: 163–1176
Guilbault GG (1990) Practical fluorescence, 2nd ed. Marcel Dekker New York
Holland HD, Gottfried D (1955) The effect of nuclear radiation on the structure of zircon. Acta Crystallogr 8: 291–300
Judd BR, Runciman WA (1976) Transverse Zeeman effect for ions in uniaxial crystals. Proc Roy Soc Lond (A)352: 91–108
Lakowicz JR (1983) Principles of fluorescence spectroscopy. Plenum New York, 496 pp
Mackey DJ, Runciman WA, Vance ER (1975) Crystal calculations for energy levels of U4+ in ZrSiO4. Phys Rev 155: 262–267
Murakami T, Chakoumakos BC, Ewing RC, Lumpkin GR, Weber WJ (1991) Alpha-decay event damage in zircon. Am Mineral 76: 1510–1532
Nasdala L, Irmer G, Wolf D (1995) The degree of metamictization in zircon: a Raman spectroscopic study. Eur J Mineral 7: 471–478
Nasdala L, Wenzel M, Vavra G, Irmer G, Wenzel T, Kober B (2001) Metamictisation of natural zircon: accumulation versus thermal annealing of radioactivity-induced damage. Contrib Mineral Petrol 141: 125–144
Richman I, Kisliuk P, Wong EY (1967) Absorption spectrum of U4+ in zircon (ZrSiO4). Phys Rev 155: 262–267
Ríos S, Salje EKH, Zhang M, Ewing RC (2000) Amorphization in natural zircon: evidence for direct impact damage. J Phys: Condens Matter 12: 2401–2412
Salje EKH, Chrosch J, Ewing RC (1999) Is "metamictization" of zircon a phase transition? Am Mineral 84: 1107–1116
Vance ER, Mackey DJ (1974) Optical study of U5+ in zircon. J Phys C: Solid State Phys 7: 1898–1909
Vance ER, Mackey DJ (1975) Further studies of the optical absorption spectrum of U4/5+ in zircon. J Phys C: Solid State Phys 8: 3439–3447
Vance ER, Mackey DJ (1978) Optical spectra of U4+ and U5+ in zircon, hafnon, and thorite. Phys Rev 18: 185–189

Weber WJ, Ewing RC, Catlow CRA, de la Rubia TD, Hobbs LW, Kinoshita C, Matzke H, Motta AT, Nastasi M, Salje EHK, Vance ER, Zinkle SJ (1998) Radiation effects in crystalline ceramics for the immobilization of high-level waste and plutonium. J Mat Res 13: 1434–1484

Woodhead JA, Rossman GR, Silver LT (1991) The metamictization of zircon: radiation dose-dependent structural characteristics. Am Mineral 76: 74–82

Zhang M, Salje EKH (2001) Infrared spectroscopic analysis of zircon: radiation damage and the metamict state. J Phys: Condens Matter 13: 3057–3071

Zhang M, Salje EKH, Ewing RC (2003) Oxidation state of uranium in metamict and annealed zircon: near-infrared spectroscopic quantitative analysis. J Phys: Condens Matter 15: 3445–3470

Zhang M, Salje EKH, Ewing RC (2002) IR Spectra of Si–O overtones, hydrous species and U ions in metamict zircon: radiation damage and recrystallization. J Phys: Condens Matter 14: 3333–3352

Zhang M, Salje EKH, Capitani GC, Leroux H, Clark AM, Schlüter J (2000a) Annealing of α-decay damage in zircon: a Raman spectroscopic study. J Phys: Condens Matter 12: 3131–3148

Zhang M, Salje EKH, Ewing RC, Farnan I, Ríos S, Schlüter J, Leggo P (2000b). α-decay damage and recrystallization in zircon: evidence for an intermediate state from infrared spectroscopy. J Phys: Condens Matter 12: 5189–5199

Zhang M, Salje EKH, Farnan I, Graem-Barber A, Danial P, Ewing RC, Clark AM, Leroux H. (2000c) Metamictization of zircon: Raman spectroscopic study. J Phys: Condens Matter 12: 1915–1925